Magnetic phase diagram of the S=1 axial next-nearest-neighbour Ising (ANNNI) model with higher-order spin interaction

1994 J. Phys. A: Math. Gen. 27 2675

(http://iopscience.iop.org/0305-4470/27/8/007)

J. Phys. A: Math. Gen. 27 (1994) 2675–2686. Printed in the UK

Magnetic phase diagram of the $S = 1$ axial next-nearest-neighbour Ising (ANNNI) model with higher-order spin interaction

Y Muraoka†, M Ochiai‡ and T Idogaki‡

† Department of General Education, Ariake National College of Technology, Omuta, Fukuoka 386, Japan

‡ Department of Applied Science, Faculty of Engineering 36, Kyushu University, Fukuoka 812, Japan

Received 10 August 1993, in final form 20 December 1993

Abstract. The three-dimensional $S = 1$ axial next-nearest-neighbour Ising (ANNNI) model is discussed. In addition to the ferromagnetic intra- and interlayer interactions J_0 and J_1 two types of competing antiferromagnetic interactions are considered between next-nearest layers, i.e. ordinary two-site two-spin $J_2 S_i S_{i+2}$ ([2–2] model) or three-site four-spin $J_3 S_i S_{i+1}^2 S_{i+2}$ ([3–4] model) interactions. For both models, the magnetic phase diagrams are obtained by means of the site-dependent molecular field approximation. The phase boundaries among paramagnetic, ferromagnetic and various modulated phases are determined by analysing frequency-dependent susceptibility $\chi(q)$, or by solving coupled equations of $\langle S_i \rangle$ and $\langle S_i^2 \rangle$ for spins up to 17, iteratively. The constructed 'devil's flower' of the [3–4] model is characteristically different from that of the [2–2] model, since three-site four-spin interaction is effectively temperature-dependent. For the [3–4] model, a new behaviour of re-entrant transition is found for the interaction ratio $-0.50 > J_3/J_1 > -0.53$. The role of the entropy term for this re-entrant transition is discussed in detail by analysing the free energies around the multiphase point ($T = 0$, $J_3/J_1 \simeq -0.5$).

1. Introduction

The systems with competing interactions represent the various types of phase transition and ordered states, and have attracted many investigators. The axial next-nearest-neighbour Ising (ANNNI) model is one of several very attractive systems. This model was originally introduced to describe the spatially modulated phases which can be either commensurate or incommensurate with the underlying lattice [1, 2]. The theoretical studies [3–8] performed for the three-dimensional $S = \frac{1}{2}$ system have revealed interesting properties such as 'the devil's flower and staircase'. The spin quantum number dependence of the ANNNI model remains an interesting problem.

Although ANNNI models seem to be too simple to describe specific materials quantitatively, they reproduce crucial quantitative features observed experimentally in adsorbate systems, ferroelectrics, magnetic systems, alloys and so on which exhibit modulated structures [9]. On the other hand, the ordinary ANNNI model does not explain the existence of zero magnetization layers (partially disordered phase) observed in CeSb [2] and $PrCo_2Si_2$ [10].

In the case of $S \geqslant 1$, it is known that the higher-order spin interactions, $S_i^2 S_j^2$, $S_i S_j^2 S_k$ and so on, become important as well as the ordinary bilinear exchange interaction, $S_i S_j$ [11, 12].

0305-4470/94/082675+12$19.50

These interactions strongly affect the phase transition, and the Blume–Emery–Griffiths (BEG) model [13] and the Blume–Capel model [14] are well known as typical systems. Although the ordinary ANNNI model has not fully succeeded in explaining the partially disordered phase, it may be possible to explain the experimental results by introducing the higher-order spin interactions.

In a previous paper [15], based on the transfer matrix method and Monte Carlo simulation, we have discussed the ground state and the order–disorder transition for two types of the three-dimensional $S = 1$ ANNNI model, described by the following Hamiltonian:

$$H = -J_0 \sum_{\langle i,j \rangle}^{nn} S_i S_j - J_1 \sum_{\langle i,j \rangle}^{nn} S_i S_j - J_2 \sum_{\langle i,j \rangle}^{nnn} S_i S_j \qquad \text{[2–2] model} \tag{1}$$

$$H = -J_0 \sum_{\langle i,j \rangle}^{nn} S_i S_j - J_1 \sum_{\langle i,j \rangle}^{nn} S_i S_j - J_3 \sum_{\langle i,j,k \rangle}^{nnn} S_i S_j^2 S_k \qquad \text{[3–4] model} \tag{2}$$

where $S_i = \pm 1$ or 0, $J_0 > 0$ is a ferromagnetic nearest-neighbour interaction within the xy plane, and $J_1 > 0$ and $J_{2(3)} < 0$ are competing interactions between nearest and next-nearest (or three adjacent) layers perpendicular to the z-direction, respectively (figure 1).

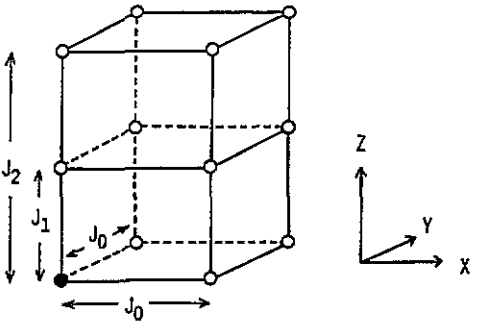

Figure 1. The three-dimensional ANNNI model.

For both models, the ground state has been rigorously obtained by means of the transfer matrix method, and proved to change from ferromagnetic to antiphase spin structure at $\kappa_{2(3)} = J_{2(3)}/J_1 = -\frac{1}{2}$ with the increase of competition. This result is in agreement with that of the ordinary $S = \frac{1}{2}$ ANNNI model [4].

From magnetization, internal energy, specific heat and 'absolute magnetization' calculated by the Monte Carlo simulation with Fourier transformation, phase boundaries among the paramagnetic, the ferromagnetic and the modulated phases were determined with the location of the Lifshitz point (LP). In the vicinity of the paramagnetic phase transition, the correlation along the z-direction becomes considerably weaker than the correlation in the xy plane owing to the frustration along the z-direction. It was concluded that for both [2–2] and [3–4] models there exists a temperature region in which the system behaves as a quasi-two-dimensional system, while for the [3–4] model the self-spin correlation, S_{i+1}^2, included in the three-site four-spin interaction, somewhat weakens the frustration between J_1 and J_3 at high temperatures.

It was difficult to use the Monte Carlo algorithm to probe the detailed structures of the modulated phases, due to the impossibility of choosing a lattice size and boundary

condition along the axial direction which do not affect the periodicity of the modulation. The modulated structures, therefore, remain as an interesting problem to be studied. In this paper, by means of the site-dependent molecular field calculation, the details of the modulated spin structures are investigated. The phase diagram for the [3–4] model shows that there exists the re-entrant phase transition for $-0.53 < \kappa_3 < -0.50$. This re-entrant phase transition is discussed by analytically calculating and comparing the free energies of the ferromagnetic, modulated and antiphase states in the vicinity of the multiphase point.

The arrangement of the paper is as follows. In section 2, based on the site-dependent molecular field approximation, the thermal averages, free energy and the transition temperatures are derived. In section 3, by means of numerical calculation, the phase diagrams for [2–2] and [3–4] models are obtained. In section 4, the cause of the re-entrant phase transition is discussed. Finally, in section 5 the results are summarized and concluding remarks given.

2. The site-dependent molecular field approximation

We consider the three-dimensional $S = 1$ ANNNI model described by the following Hamiltonian:

$$H = -\sum_{\langle ij \rangle} J_{ij} S_i S_j - \sum_{\langle ijk \rangle} J_{ijk} S_i S_j^2 S_k \tag{3}$$

where J_{ij} denotes J_0, J_1 or J_2 in figure 1, and J_{ijk} denotes the three-site four-spin interaction J_3 along the z-axis. For $J_3 = 0$ or $J_2 = 0$, this Hamiltonian corresponds to the [2–2] or [3–4] model, respectively. In terms of thermal averages $\langle S_i \rangle$ and $\langle S_i^2 \rangle$, S_i and S_i^2 are expressed as

$$S_i = \langle S_i \rangle + (S_i - \langle S_i \rangle) \tag{4}$$

$$S_i^2 = \langle S_i^2 \rangle + (S_i^2 - \langle S_i^2 \rangle). \tag{5}$$

Neglecting higher orders of fluctuation for S_i and S_i^2, the Hamiltonian in the molecular field approximation is obtained as follows:

$$H_{\mathrm{MF}} = -\sum_j (S_j h_j + S_j^2 h_j^* - \tfrac{1}{2}\langle S_j \rangle h_j - \langle S_j^2 \rangle h_j^*) \tag{6}$$

where

$$h_j = \sum_i J_{ij} \langle S_i \rangle + \sum_{i,k} J_{ijk} \langle S_i^2 \rangle \langle S_k \rangle \tag{7}$$

$$h_j^* = \sum_{\langle ik \rangle} J_{ijk} \langle S_i \rangle \langle S_k \rangle. \tag{8}$$

From equations (6), (7) and (8), the thermal averages of S_i and S_i^2,

$$\langle S_j \rangle = \frac{2\exp(\beta h_j^*)\sinh(\beta h_j)}{1 + 2\exp(\beta h_j^*)\cosh(\beta h_j)} \tag{9}$$

$$\langle S_j^2 \rangle = \frac{2\exp(\beta h_j^*)\cosh(\beta h_j)}{1 + 2\exp(\beta h_j^*)\cosh(\beta h_j)} \tag{10}$$

and free energy per spin,

$$F = \frac{1}{N}\sum_{j}^{N}\left\{-T\log[2\exp(\beta h_j^*)\cosh(\beta h_j)+1] + \frac{1}{2}\langle S_j\rangle h_j + \langle S_j^2\rangle h_j^*\right\} \quad (11)$$

are obtained, where $\beta = 1/T$. The Boltzmann constant is taken to be unity.

In the paramagnetic state, the induced $\langle S_j\rangle$ and $\langle S_j^2\rangle$ under the site-dependent external field H_j are calculated from equations (9) and (10), and are given by neglecting higher orders of h_j, h_j^* and H_j as follows:

$$\langle S_j\rangle \approx a\beta(h_j - g\mu_B H_j) \quad (12)$$

$$\langle S_j^2\rangle \approx a(1+\beta h_j^*) \quad (13)$$

where $a = S(S+1)/3 = \frac{2}{3}$ for $S = 1$, and g and μ_B denote the g-factor and Bohr magneton, respectively.

Now, we introduce the Fourier components of $\langle S_j\rangle$ and the site-dependent external field H_j,

$$\langle S_j\rangle = \sum_q \langle S_q\rangle \exp(\mathrm{i}q\cdot r_j) \quad (14)$$

$$H_j = \sum_q H_q \exp(\mathrm{i}q\cdot r_j). \quad (15)$$

Equations (12)–(15) give

$$\langle S_q\rangle = \frac{a}{T}[(J(q) + a\tilde{J}(q))\langle S_q\rangle - g\mu_B H_q] \quad (16)$$

where $J(q)$ and $\tilde{J}(q)$ denote the Fourier components of the two-site two-spin type interaction and the three-site four-spin type interaction, respectively, described by

$$J(q) = \sum_i J_{ij}\exp[\mathrm{i}q\cdot(r_j - r_i)] \quad (17)$$

$$\tilde{J}(q) = \sum_{i,k} J_{jik}\exp[\mathrm{i}q\cdot(r_j - r_k)]. \quad (18)$$

From equation (16), the wavevector-dependent susceptibility $\chi(q) = -Ng\mu_B\langle S_q\rangle/H_q$ is given by

$$\chi(q) = \frac{C}{T - T(q)} \quad (19)$$

where

$$C = Na(g\mu_B)^2 \quad (20)$$

$$T(q) = a[J(q) + a\tilde{J}(q)]. \quad (21)$$

From equations (17) and (18), equation (21) is written as

$$T(q) = a[2J_0(\cos q_x + \cos q_y) + 2J_1 \cos q_z + 2J_2 \cos 2q_z + 2aJ_3 \cos 2q_z] \tag{22}$$

where the lattice constant is taken to be unity. With the decrease of temperature from the paramagnetic state, the ordered state corresponding to the critical wavevector q_c, for which equation (22) becomes maximal, appears at the beginning. For the fixed value of $\kappa_0 = J_0/J_1 > 0$ and $\kappa = \kappa_2 + a\kappa_3 < 0$, we calculate the critical wavevector $q_c(q_x^c, q_y^c, q_z^c)$. In the case of $-\frac{1}{4} < \kappa < 0$, $q_x^c = q_y^c = q_z^c = 0$ (the ferromagnetic phase or F-phase) and in the case of $\kappa < -\frac{1}{4}$, $q_x^c = q_y^c = 0$ and $q_z^c = \cos^{-1}(-\frac{1}{4}\kappa)$ (the modulated phase or M-phase) are obtained. If $T(q_c)$ for each case is symbolized by T_c and T_m, respectively, then we get

$$\frac{T_c}{aJ_1} = 4\kappa_0 + 2(1+\kappa) \qquad (-\tfrac{1}{4} < \kappa < 0) \tag{23}$$

$$\frac{T_m}{aJ_1} = 4\kappa_0 - 2\left(\kappa + \frac{1}{8\kappa}\right) \qquad (\kappa < -\tfrac{1}{4}). \tag{24}$$

The LP, at which the P-, F- and M-phases coexist, is given by

$$\kappa^* = -\tfrac{1}{4} \qquad \frac{T^*}{aJ_1} = 4\kappa_0 + \tfrac{3}{2}. \tag{25}$$

The Lifshitz temperature T^* is common for both models, but this is not the case for κ_2^* and κ_3^*. For the [2–2] model ($\kappa_3 = 0$), the ratio of the competing interactions at the LP is $\kappa_2^* = -\frac{1}{4}$ and is not concerned with the spin value S. For the [3–4] model ($\kappa_2 = 0$), however, κ_3^* is proportional to $a \propto S(S+1)$ and has the smaller value of $\kappa_3^* = -\frac{3}{8}$ compared with $\kappa_2^* = -\frac{1}{4}$ of the [2–2] model in the present case of $S = 1$. This shift of the LP is due to the self-spin correlation $\langle S_j^2 \rangle$ included in the three-site four-spin interaction. For both the [2–2] and [3–4] models, T_c, T_m and LP are shown in table 1.

Table 1. T_c, T_m and LP for the $S = 1$ ANNNI model by means of the molecular field approximation, where $\kappa_0 = J_0/J_1$ and $a = S(S+1)/3 = \frac{2}{3}$.

	T_c/aJ_1	T_m/aJ_1	LP
[2–2] model	$4\kappa_0 + 2 + 2\kappa_2$	$4\kappa_0 - 2\kappa_2 - \dfrac{1}{4\kappa_2}$	$\kappa_2^* = -\frac{1}{4}$
[3–4] model	$4\kappa_0 + 2 + \dfrac{4\kappa_3}{3}$	$4\kappa_0 - \dfrac{4\kappa_3}{3} - \dfrac{3}{8\kappa_3}$	$\kappa_3^* = -\frac{3}{8}$

3. The numerical calculation

From equations (23) and (24), the phase boundary between the paramagnetic phase (P-phase) and the ordered phase (F- or M-phase) has been obtained. In the ANNNI model, as the intralayer interactions J_0 are ferromagnetic, the x- and y-components of the wavevector are always zero, corresponding to the ferromagnetic order in the layer. Therefore, the ordered state is characterized by the z-component q_z. In the following $q_z/2\pi$ is defined as q. To investigate the ordered phase, the coupled equations of equations (9) and (10) for

spins up to $N = 17$ are self-consistently solved by means of the iteration. The stable spin structure is determined as the solution which minimizes the free energy given by equation (11). In the case of $N \leqslant 17$, the spin structures corresponding to $q = 0$ and $\frac{1}{17} \leqslant q \leqslant \frac{1}{4}$ should be considered. For higher values of N, complex structures with longer periodicities appear in the phase diagrams. These structures, however, are unstable except within an extremely narrow temperature region in the phase diagram. It is believed that no additional significant insight can be achieved by extending the numerical calculation to such higher values of N [5]. Due to the small lattices ($N \leqslant 17$) and the periodic boundary condition, however, only commensurate phases can be identified, and the systematics of the high-order commensurate phases are missed. To make up for these defects, it is necessary to do more sophisticated analyses of the mean-field equations, in particular following Selke and Duxbury [16].

The dependences of the critical wavevector q_c on $\kappa_{2(3)}$ for two models are shown in figure 2. The change of the wavevector with temperature is larger in the [3–4] model than in the [2–2] model. As $\kappa_{2(3)} \to -\infty$, q_c approaches the $\frac{1}{4}$ antiphase (A-phase) in both models.

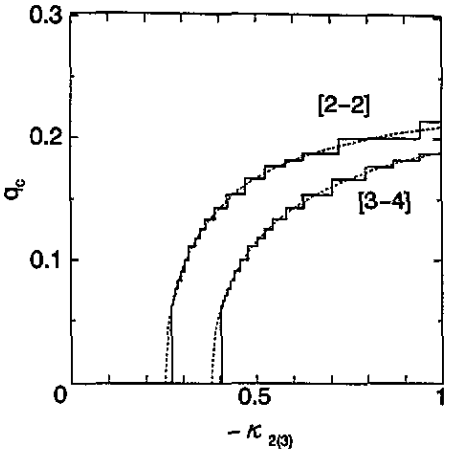

Figure 2. The dependence of the critical wavevector q_c on $\kappa_{2(3)}$ for the [2–2] and [3–4] models. The full lines denote the numerical calculation for $N \leqslant 17$. The broken lines denote the case of $N \to \infty$ ($q_c = \cos^{-1}(-\frac{1}{4}\kappa)$).

The T–κ magnetic phase diagrams for the [2–2] and [3–4] models are shown in figures 3 and 4, respectively. For both models, an infinite number of phases degenerate at the multiphase point, $(\kappa_{2(3)}, T) = (-\frac{1}{2}, 0)$. Figure 3 is similar to the magnetic phase diagram for the $S = \frac{1}{2}$ three-dimensional ANNNI model [5]. On the other hand, figure 4 shows that the ferromagnetic phase is extended into the modulated phase region, and for $-0.53 < \kappa_3 < -0.5$ the re-entrant phase transition (M → F → M) takes place for the [3–4] model. In previous work, the Monte Carlo simulation for $\kappa_3 = -0.52$ cannot find such a re-entrant phase transition [15]. This fact suggests that the region of the re-entrant phase transition might be more narrow. It is difficult but necessary to carry out the Monte Carlo simulation for such a critical region of $-0.52 < \kappa_3 < -0.5$.

Comparing the phase diagram for the [3–4] model (figure 4) with that of the [2–2] model (figure 3), the P–F and M–F phase transitions in [3–4] model take place on the

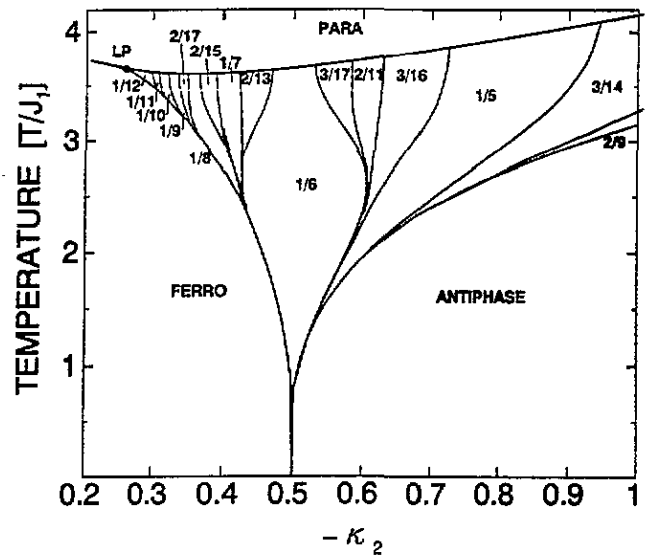

Figure 3. The magnetic phase diagram for the [2–2] model.

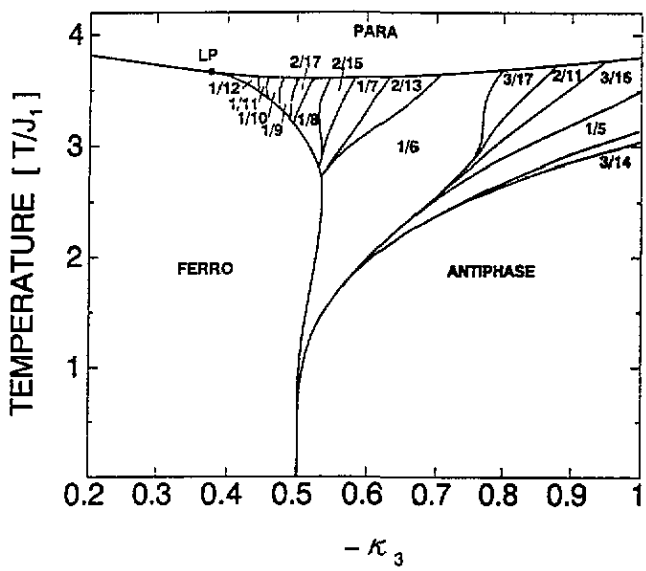

Figure 4. The magnetic phase diagram for the [3–4] model.

higher-temperature side and the P–M and M–A phase transitions take place on the lower-temperature side compared with the [2–2] model. This result is qualitatively in agreement with that of the Monte Carlo simulation [15], and is explained by the self-spin correlation S_j^2 included in the three-site four-spin interaction, $J_3 S_i S_j^2 S_k$. For the [3–4] model, the effective field, h_j, (equation (7)) includes the self-spin correlation, $\langle S_j^2 \rangle$. As the temperature is raised, $\langle S_j^2 \rangle$ decreases monotonously from 1 to $\frac{2}{3}$ and the three-site four-spin interaction, $J_3 S_i S_j^2 S_k$,

is weakened by the factor $\langle S_j^2 \rangle$ compared with the bilinear interaction, $J_2 S_i S_j$. Namely, as the temperature is raised, the frustration in the [3–4] model becomes weaker than that in the [2–2] model. Therefore, the F-phase for the [3–4] model becomes stable in the higher-temperature region than that for the [2–2] model, and the P–F and M–F phase transitions take place on the higher-temperature side. For the same reason, the A- or M-phases for the [3–4] model become unstable in the lower-temperature region than those for the [2–2] model, and the P–M and M–A phase transitions take place on the lower-temperature side. The extension of the ferromagnetic phase into the modulated phase region in the [3–4] model is also attributed to self-spin correlation. This causes the re-entrant phase transition, which is analytically investigated in the next section.

4. The re-entrant phase transition in the [3–4] model

In the [3–4] model, the weakening of the three-site four-spin interaction stabilizes the ferromagnetic phase at high temperatures. As shown in figure 4, in the vicinity of the multiphase point, $(\kappa_3, T) = (-0.5, 0)$, the leaning of the F–M phase boundary towards small κ_3 results in the re-entrant transition (A → M → F → M → P) in $-0.53 < \kappa_3 < -0.5$. In this section, the cause of the re-entrant phase transition is discussed by analytically calculating and comparing the free energies of the F, A ($q = \frac{1}{4}$) and M ($q = \frac{1}{6}$) phases.

The free energy (equation (11)) can be divided into the internal energy U and the entropy S parts:

$$F = U - TS \tag{26}$$

$$U = -\frac{1}{2N} \sum_j^N h_j \langle S_j \rangle \tag{27}$$

$$S = \frac{1}{N} \sum_j^N \left\{ \log[1 + 2\exp(\beta h_j^*)\cosh(\beta h_j)] - \langle S_j \rangle \frac{h_j}{T} - \langle S_j^2 \rangle \frac{h_j^*}{T} \right\}. \tag{28}$$

From equations (9) and (10), $\langle S_j \rangle$ and $\langle S_j^2 \rangle$ can be written as follows:

$$\langle S_j \rangle = 1 - \delta_j^{(m)} \tag{29}$$

$$\langle S_j^2 \rangle = 1 - \delta_j^{(q)} \tag{30}$$

where

$$\delta_j^{(m)} = \frac{\exp[-\beta(h_j + h_j^*)] + 2\exp(-2\beta h_j)}{1 + \exp[-\beta(h_j + h_j^*)] + \exp(-2\beta h_j)} \tag{31}$$

$$\delta_j^{(q)} = \frac{\exp[-\beta(h_j + h_j^*)]}{1 + \exp[-\beta(h_j + h_j^*)] + \exp(-2\beta h_j)}. \tag{32}$$

Around the multiphase point, it is easy to show $\delta_j \equiv \delta_j^{(m)} \approx \delta_j^{(q)} \approx \exp(-\beta h_j)$ for the [2–2] model and $\delta_j \equiv \delta_j^{(m)} \approx \delta_j^{(q)} \approx \exp[-\beta(h_j + h_j^*)]$ for the [3–4] model. At low

temperatures, the free energy for both models can be represented as follows by using δ_j defined above:

$$F = -\frac{1}{2N}\sum_j (1-\delta_j)h_j - \frac{T}{N}\sum_j (\delta_j - \delta_j \log \delta_j). \tag{33}$$

To compare the free energies for the three different phases, we denote δ_j as δ_F in the F-phase, δ_A in the A-phase and δ_1 or δ_2 in the M ($q = \frac{1}{6}$) phase since there exist two kinds of spin in this phase (figure 5). If we estimate the strength of h_j (and h_j^*) for each phase after some lengthy calculations we found

$$[2\text{–}2] : \delta_2 \approx \exp(-4\beta J_1) \gg \delta_F, \delta_A, \delta_1 \tag{34}$$

$$[3\text{–}4] : \delta_2 \approx \delta_F \approx \exp(-\tfrac{9}{2}\beta J_1) \gg \delta_A, \delta_1. \tag{35}$$

In equation (33), therefore, all other δ_j except for δ_2 and except for both δ_2 and δ_F can be neglected for the [2–2] and [3–4] models, respectively.

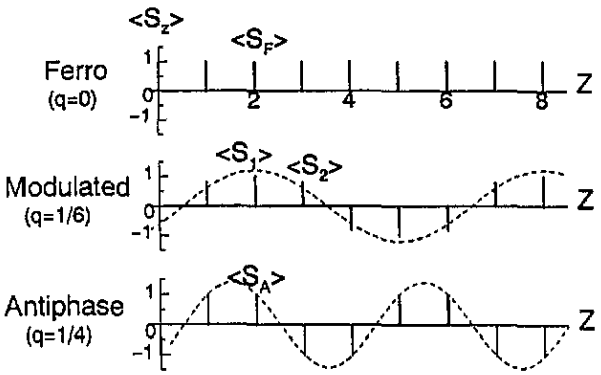

Figure 5. The spin structures along the z-axis in the F, M ($q = \frac{1}{6}$) and A ($q = \frac{1}{4}$) phases.

In the vicinity of the multiphase point, $\kappa_{2(3)}$ can be written as $\kappa_{2(3)} = -0.5 - \Delta$ ($\Delta \ll 1$), and the free energy per spin in each phase are given by:

[2–2] model

$$F_F \approx -\frac{J_1}{2}(5 - 2\Delta) \tag{36a}$$

$$F_M \approx -\frac{J_1}{6}(15 + 2\Delta - 16\delta_2) - \tfrac{2}{3}T(\delta_2 - \delta_2 \log \delta_2) \tag{36b}$$

$$F_A \approx -\frac{J_1}{2}(5 + 2\Delta) \tag{36c}$$

[3–4] model

$$F_F \approx -\frac{J_1}{2}(5 - 2\Delta - 9\delta_F) - T(\delta_F - \delta_F \log \delta_F) \tag{37a}$$

$$F_M \approx -\frac{J_1}{6}(15 + 2\Delta - 18\delta_2) - \tfrac{2}{3}T(\delta_2 - \delta_2 \log \delta_2) \tag{37b}$$

$$F_A \approx -\frac{J_1}{2}(5 + 2\Delta). \tag{37c}$$

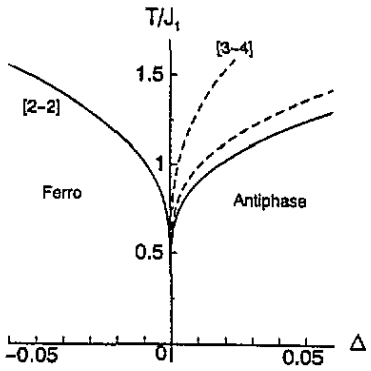

Figure 6. The magnetic phase diagram around the multiphase point. There exists an M-phase between the full lines for the [2–2] model and between the broken lines for the [3–4] model, respectively. Δ is defined as $\kappa_{2(3)} = -0.5 - \Delta$.

Comparing the free energies of each phase, the phase boundaries are determined as follows:

[2–2] model

$$\text{F–M} : \Delta \approx -\frac{T}{2J_1}\delta_2 \approx -\frac{T}{2J_1}\exp(-4J_1/T) \tag{38}$$

$$\text{A–M} : \Delta \approx \frac{T}{J_1}\delta_2 \approx \frac{T}{J_1}\exp(-4J_1/T) \tag{39}$$

[3–4] model

$$\text{F–M} : \Delta \approx \frac{3T}{4J_1}\left(-\frac{2}{3}\delta_2 + \delta_F\right) \approx \frac{T}{4J_1}\exp(-9J_1/2T) \tag{40}$$

$$\text{A–M} : \Delta \approx \frac{T}{J_1}\delta_2 \approx \frac{T}{J_1}\exp(-9J_1/2T). \tag{41}$$

Figure 6 shows the phase boundaries among three phases in the vicinity of the multiphase point. While the F–M phase boundary of the [2–2] model exists in the region of $\Delta < 0$, that of the [3–4] model exists in the region of $\Delta > 0$. Equations (38) and (40) suggest that this difference between the [2–2] and [3–4] models is attributed to the enhancement of δ_F in the [3–4] model, which is neglected in the [2–2] model. In the [2–2] model the entropy effect of δ_2 stabilizes the M-phase. In the [3–4] model, δ_F and δ_2 are of the same order. The thermal averages of only $\frac{2}{3}$ spins decrease by δ_2 in the M-phase ($q = \frac{1}{6}$) while the thermal averages of all spins decrease by δ_F in the F-phase. Therefore, the entropy effect stabilized the F-phase. Comparing the role of h_j and h_j^*, it is understood that h_j^* in the [3–4] model causes δ_F to be nearly equal with δ_2. The Hamiltonian in the molecular field approximation (equation (6)) suggests that h_j^* can be regarded as the effective field applied to S_j^2. Since $h_j^* < 0$ in the F-phase, h_j^* stabilizes the F-phase with small S_F^2, that is, the F-phase including many spins with $S_F = 0$ and having small $\langle S_F \rangle$. Then, δ_F becomes large enough not to be neglected. Consequently, the three-site four-spin interaction has the same effect as the single ion anisotropy, $DS_j^2 (D > 0)$, and the increase of the entropy in the F-phase by this effect results in the re-entrant phase transition in the [3–4] model.

5. Conclusions

We have studied the magnetic phase diagrams for both $S = 1$ [2–2] and $S = 1$ [3–4] models in three dimensions, based on the site-dependent molecular field approximation. The results in this paper complement the previous work by Monte Carlo simulation.

To investigate the ordered phase, the coupled equations for spins up to $N = 17$ are self-consistently solved by means of the iteration. The stable spin structure is determined as the solution which minimizes free energy among the solutions of the coupled equation, and the magnetic phase diagrams are obtained for both models. For the [3–4] model, the P–F and M–F phase transitions take place on the higher-temperature side and the P–M and M–A phase transitions take place on the lower temperature side compared with the [2–2] model. This result is qualitatively in agreement with that of the previous Monte Carlo simulation [15] and is attributed to the temperature dependence of the self-spin correlation S_j^2 included in the three-site four-spin interaction. While the phase diagram of the [2–2] model is similar to that of the usual $S = \frac{1}{2}$ ANNNI model, the phase diagram of the [3–4] model shows the re-entrant phase transition for $-0.53 < \kappa_3 < -0.50$.

The re-entrant phase transition is discussed by analytically calculating and comparing the free energies of ferromagnetic, modulated ($q = \frac{1}{6}$) and antiphase ($q = \frac{1}{4}$) states in the vicinity of the multiphase point. It is confirmed that the three-site four-spin interaction has the same effect as the single ion anisotropy, $DS_j^2 (D > 0)$, and the increase of the entropy in the ferromagnetic phase by this effect stabilizes the ferromagnetic phase and results in the re-entrant phase transition in the [3–4] model.

A similar system with the higher-order spin interaction has been studied by Jensen *et al* [17]. Their Hamiltonian includes the term $-K[S_i^2(1 - S_{i+1}^2) + (1 - S_i^2)S_{i+1}^2]$ in addition to equation (1). Due to this term, the combination of $S_i = 0$ between two neighbouring $|S_{i\pm1}| = 1$ terms is energetically favourable. This system shows a similar re-entrant phase transition to the [3–4] model, which is due to the bulge of the ferromagnetic phase into the modulated region. The stabilization of the ferromagnetic phase at high temperatures may also be attributed to the entropy effect by the added term.

In this paper, both the [2–2] and [3–4] models were restricted to the case of $J_0 = J_1$. In the mean-field theory of the $S = \frac{1}{2}$ three-dimensional ANNNI model, Yokoi studied the effect of the weakening of the intralayer interactions, J_0, and showed that there existed commensurate phases with disordered layers (partially disordered phase) and that commensurate phases, which lack the usual reflection or inversion symmetries, might be stabilized [18]. Recently, Nakanishi showed that in the ordinary $S = \frac{1}{2}$ ANNNI model neither the partially disordered phases nor the asymmetric phases are stabilized, and only the conventional ordered states are stable, by means of the modified mean field theory, which exactly treats the competing axial interactions [19]. A Monte Carlo study by Rotthaus and Selke supports Nakanishi's results [20]. For the $S = 1$ [2–2] and [3–4] models, the possibilities of the partially disordered phase and the asymmetric phase by the weakening of the intralayer interactions, J_0, are not investigated. It is known that the spin quantum number, S, largely affects the higher-order spin interactions compared with the ordinary bilinear interaction. The dependence of the magnetic phase diagram on the spin quantum number remains an interesting problem.

Acknowledgments

The authors would like to express their sincere thanks to Professors N Uryû and K Takeda for their valuable discussions.

References

[1] Elliot R J 1961 *Phys. Rev.* 124 346–53
[2] Rossat-Mignod J, Burlet P, Bartholin H, Vogt O and Lagnier R 1980 *J. Phys. C: Solid State Phys.* **13** 6381–9
[3] Render S and Stanley H E 1977 *J. Phys. C: Solid State Phys.* **10** 4765–84
[4] Selke W and Fisher M E 1979 *Phys. Rev.* B **20** 257–65
[5] Bak P and von Boehm J 1980 *Phys. Rev.* B **21** 5297–308
[6] Fisher M E and Selke W 1980 *Phys. Rev. Lett.* **44** 1502–5
[7] Yokoi C S O, Coutinho-Filho M D and Salinas S R 1981 *Phys. Rev.* B **24** 4047–61
[8] Oitmaa J 1985 *J. Phys. A: Math. Gen.* **18** 365–75
[9] Selke W 1988 *Phys. Rep.* **170** 213–64
[10] Takeda T, Konishi K, Deguchi H, Iwata N and Shigeoka T 1992 *J. Magn. Magn. Mater.* **104–107** 901–2
[11] Iwashita T and Uryû N 1979 *J. Phys. Soc. Japan* **47** 786–9
[12] Idogaki T and Uryû N 1985 *Phys. Lett.* **110A** 467–9
[13] Blume M, Emery V J and Griffiths R B 1971 *Phys. Rev.* A 4 1071–7
[14] Blume M 1966 *Phys. Rev.* **141** 517–24
[15] Muraoka Y, Ochiai M, Idogaki T and Uryû N 1993 *J. Phys. A: Math. Gen.* **26** 1811–21
[16] Selke W and Duxbury P M 1984 *Z. Phys.* B **57** 49–58
[17] Jensen P J, Penson K A and Bennemann K H 1987 *Phys. Rev.* B **35** 7306–9
[18] Yokoi C S O 1991 *Phys. Rev.* B **43** 8487–90
[19] Nakanishi K 1992 *J. Phys. Soc. Japan* **61** 2901–8
[20] Rotthaus F and Selke W 1993 *J. Phys. Soc. Japan* **62** 378–9